# Graphite-bearing and Graphite-depleted Basement Rocks in the Dufferin Lake Zone, South-central Athabasca Basin, Saskatchewan

Marjolaine Pascal, Kevin M. Ansdell, and Irvine R. Annesley
*Department of Geological Sciences, University of Saskatchewan, 114 Science Place, Saskatoon, Saskatchewan, S7N 5E2 (kevin.ansdell@usask.ca)*

## Abstract

Unconformity-type uranium deposits from the Athabasca Basin are interpreted to be the result of mixing between oxidized basinal brines and basement-derived reduced fluids/gases, and/or reduced basement rocks. Graphite and/or its breakdown products may be responsible for uranium mineralization by acting as a reductant that could trigger deposition of uranium. Also, graphite is considered to be indicative of basement structures as it is often concentrated along structures which can be identified as electromagnetic conductors. Underlying the sedimentary rocks of the basin in the Dufferin Lake zone (south-central Athabasca Basin) are variably graphitic pelitic schists (VGPS), which are altered to chlorite and hematite (Red/Green Zone: RGZ), and locally bleached (BZ) near the unconformity. These "graphite-depleted zones" contain rocks which are similar in texture to the VGPS, and are assumed to have contained graphite prior to alteration. The major element composition of the VGPS and RGZ are similar, but the RGZ and BZ are characterized by lower concentrations of carbon and sulphur. The BZ also has higher concentrations of uranium and boron. Raman analyses indicate that well-ordered carbon species (graphite to semi-graphite) are present in the VGPS, with both types more common within shear zones. In contrast, only rare low-ordered carbon species (carbonaceous matter) were detected in the graphite-depleted samples within the RGZ. Secondary fluid inclusions (FI) examined in different quartz vein generations provide an indication of the fluids that have interacted with the basement rocks. Monophase vapor, dominated by $CH_4$ and $N_2$ as identified by Raman, are the most common type of fluid inclusion in the VGPS, whereas aqueous two-phase (L+V) and three-phase (L+V+Halite) FI occur in the RGZ. The latter are rich in NaCl and $CaCl_2$ and are similar to brines identified elsewhere in the basin.

Overall, several events are considered to be potentially responsible for graphite consumption. However, the most important processes likely occurred during retrograde metamorphism, and during fluid-rock interactions that ultimately created the RGZ and BZ. $CH_4$ can be generated by the breakdown of graphite during hydration reactions and/or cooling of C-O-H fluids, and $N_2$ could have been generated by the breakdown of ammonium ($NH_4^+$)-bearing feldspar and micas. Basinal brines that circulated through the RGZ could also have broken down graphite and sulphides, and released gases/fluids into the sedimentary rocks of the basin. However, the absolute timing of graphite consumption is not known, and so the direct link with uranium deposition remains unclear.

## Introduction

The Athabasca Basin is located in northern Saskatchewan, Canada. It hosts the highest grade unconformity-type uranium deposits in the world, which are mainly located in the eastern part of the basin. Uranium mineralization and associated alteration are often concentrated where structures intersect the unconformity between the basin and the underlying basement rocks (Fig. 1).

Different geochemical and geophysical methods (summarized in Jefferson et al., 2007) are used to target uranium mineralization and one of the most important is determining the location of strong electromagnetic (EM) conductors. These EM conductors are often associated with graphite-rich basement rocks (Madore and Annesley, 1997; Thomas et al., 2000), because graphite is a highly conductive mineral. Graphitic conductors are often associated with shear zones/fault zones, which may provide the structural controls on fluid flow and ultimately focus precipitation of uranium minerals (Madore and Annesley, 1997; Thomas et al., 2000). In addition to acting as a conduit for fluids, graphite (s.s.) has been proposed to act as a reductant for uranium mineralization, by reacting with water to produce methane ($CH_4$) and carbon dioxide ($CO_2$) (Hoeve and Sibbald, 1978).

## Geology of the Dufferin Lake Zone

The Dufferin Lake Zone is located in the south-central part of the Athabasca Basin, spatially associated with the southern-most part of the Snowbird Tectonic Zone, a 4.5 km wide zone of cataclasites and mylonites (Gilboy, 1985a) named the Virgin River shear zone (VRSZ) (Hoffman, 1990). This forms the boundary between the Mudjatik Domain to the east and the Taltson Domain to the west (Fig.1). The VRSZ was reactivated after the deposition of the Athabasca Group as a northwest-dipping reverse fault, named the Dufferin Lake fault, which offsets the unconformity by over 250 metres (Card et al., 2007; Powell et al., 2007). This fault probably had an important role in the development of uranium mineralization in the area, as it appears to have acted as a fluid conduit over an extended period of time (Thomas et al., 2000). The basement rocks in the Mudjatik Domain are composed mainly of felsic gneisses (Gilboy, 1985a) with lesser quartzites, pelitic and variably graphitic metasedimentary rocks, and deformed amphibolites, granitoids, and pegmatites that have been metamorphosed to upper greenschist to amphibolite grade. The basement rocks in the Taltson Domain consist mainly of orthogneisses (dominated by granodiorite compositions), that have been metamorphosed to granulite-facies in its northwest part and amphibolite-facies near the VRSZ (Card

Pascal, M., Ansdell, K.M., and Annesley, I.R., 2015. Graphite-bearing and Graphite-depleted Basement Rocks in the Dufferin Lake Zone, South-central Athabasca Basin, Saskatchewan, *in* Targeted Geoscience Initiative 4: unconformity-related uranium systems, (ed.) E.G. Potter and D.M. Wright; Geological Survey of Canada, Open File 7791, p. 83–92. doi:10.4095/295776

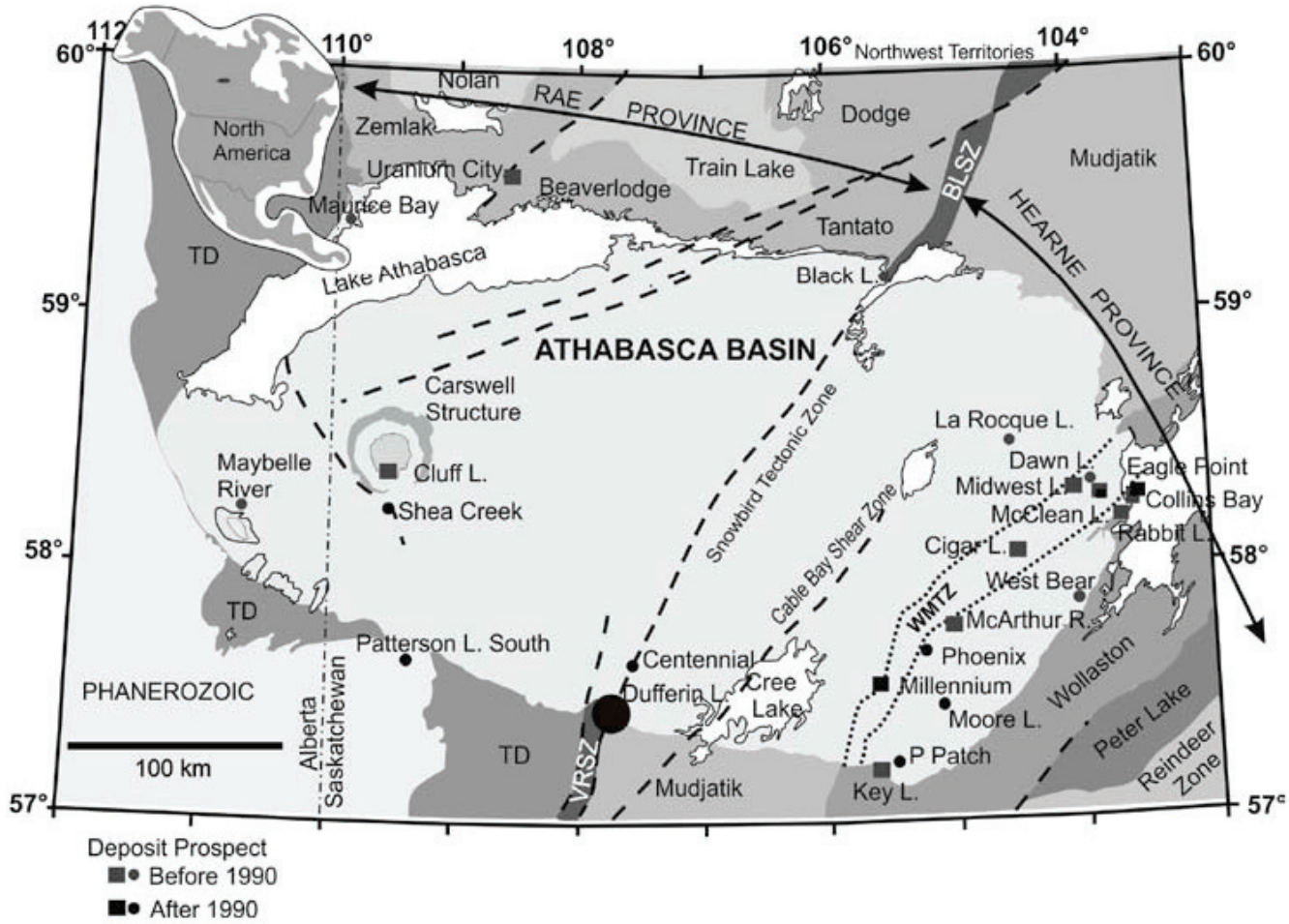


**Figure 1.** Simplified geological map of the Athabasca Basin and underlying tectonic domains (northern Saskatchewan and Alberta), showing the location of unconformity-associated uranium deposits and occurrences of the Athabasca Basin region of northwestern Canada (modified after Jefferson et al., 2007; Card, 2012). Heavy dashed lines are selected major reactivated fault zones. TD: Taltson Domain, WMTZ: Wollaston Mudjatik transition zone, VRSZ: Virgin River Shear Zone, BLSZ: Black Lake Shear Zone.

et al., 2008).

Graphitic-rich EM conductors are present in the study area, parallel to the Dufferin Lake fault (Jiricka et al., 2007). In the DLZ, uranium mineralization (Jiricka et al., 2007) is hosted in quartz-rich arenites of the Manitou Falls Formation (Fig. 2) just above (5 to 10 m) the unconformity and is associated with bleaching and clay alteration. The basement rocks directly underlying the DLZ are composed primarily of variably graphitic (locally sulphidic) pelitic schists (VGPS), with a strong sub-vertical foliation, and cut by numerous shear zones. The rocks in the red/green zone (RGZ) have the same metamorphic textures and structures, but contain no graphite, suggesting that the graphite had been removed by some process. The graphite depletion zone is composed of the RGZ and a bleached zone (Fig. 2). The lower part of the RGZ is more chloritic (green zone) and progressively becomes enriched in hematite to form the red zone in the upper part of the RGZ. This profile is interpreted to be the result of paleoweathering (Macdonald, 1980, 1985). However, this model has been modified to incorporate the circulation of basinal brines into the basement rocks (Cuney et al., 2003); overprinting the original paleoweathering profile.

## Objectives

In this study, we examined the variably graphitic pelitic schists and their altered equivalents depleted in graphite and sulphides, in order to observe and document the consumption of these minerals and to characterize the carbon species present in the graphitic samples. The purpose of this project was to document the consumption of graphite in the basement rocks and to determine how and under what conditions it has been removed. An additional aim was to determine the possible relationship between graphite and/or its breakdown in the uranium mineralizing process and thus, determine if the location of graphitic conductors is important for the localization of a deposit. A summary of the results of this study are provided in this report, and more detailed discussion is available in Pascal (2014).

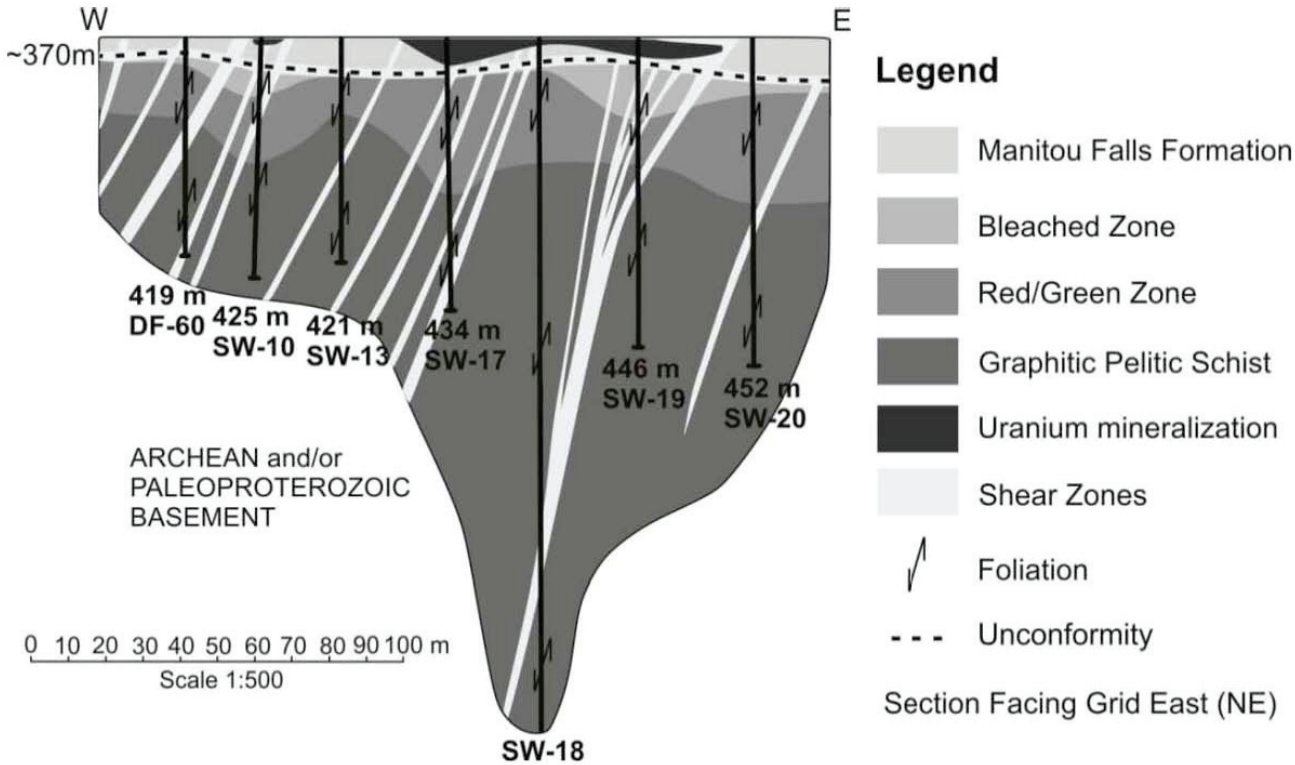


**Figure 2.** Geological cross section along grid line L250E, illustrating the presence of graphite-depleted (bleached zone and red/green zone) and graphite-rich (variably graphitic pelitic schist) zones.

## Results

*Petrography summary*

The basement rocks are porphyroblastic to granoblastic, and variably mylonitic. The samples display a strong ductile deformation fabric comprising mainly quartz, chlorite and muscovite. The porphyroblasts, when present, are garnet, staurolite, and/or andalusite (Wallis, 1970; Gilboy, 1985b), which are always retrograded (i.e. altered and recrystallized), even within the deeper drilling intersections of the basement rocks. Pyrite occurs as disseminated grains or in late veins. The mylonitic fabric can be contorted and locally microfolded, and shows a C-S structure, rotated porphyroblasts, and quartz boudinage. Primary layering (S0) and early foliation (S1) are isoclinally folded.

In the variably graphitic pelitic schists, the carbon species are often associated with pyrite and spatially associated with quartz veins. Locally, alternating quartz-rich and graphite-rich bands are observed. The porphyroblasts (garnet, staurolite, and andalusite) are generally silicified. Some carbonates veins are present. Graphite to semi-graphite (Fig. 3a), and carbonaceous matter (CM) (Fig. 3b), can sometimes be identified using reflected light microscopy, as the reflectivity is correlated with the degree of crystallinity. Graphite, semi-graphite and CM are concentrated along the foliation, within shear zones and along younger brittle fault zones. The carbon species are very fine grained and consist of small irregular or elongate particles, that can be dispersed in the matrix or form irregular aggregates or elongated parallel to the bedding (Fig. 3).

The alteration assemblage in the RGZ consists mainly of a mixture of chlorite, and hematite (Fig. 4a), with no macroscopic graphite. However, some minor carbon species are dispersed as small grains within the chloritic fabric of the green-zone, i.e. the lower part of the RGZ (Fig. 4b). Several quartz generations overprint the original fabric (Pascal, 2014) and all the porphyroblasts are replaced by quartz or by a mixture of Mg-Fe chlorite or by hematite. It appears that carbon species are not present where both hematite and quartz have strongly overprinted the fabric. The extent of "red alteration" increases upwards through the RGZ into the hematite zone (red zone; Fig. 4c), which is composed mainly of pervasive hematite and clay minerals. In the bleached zone, overlying the red zone and just below the unconformity, the rock texture is destroyed and drill core recovery is very poor. All the original silicate minerals are replaced by kaolinite, and a mixture of Mg-Fe chlorite (Fig. 4d). This bleaching process overprinted both chlorite and hematite and thus postdates the formation of the RGZ and the red zone. This zone also contains ubiquitous hydrothermal dravite. Zircon, rutile, and goyasite occur locally. Graphite was not observed.

*Raman analysis summary*

Raman analysis provides conclusive evidence for different types (i.e. species) of graphite and carbonaceous matter in the basement rocks of the DLZ (Pascal, 2014).

Samples from the variably graphitic pelitic schists exhibit similar Raman spectra, characterized by the presence of

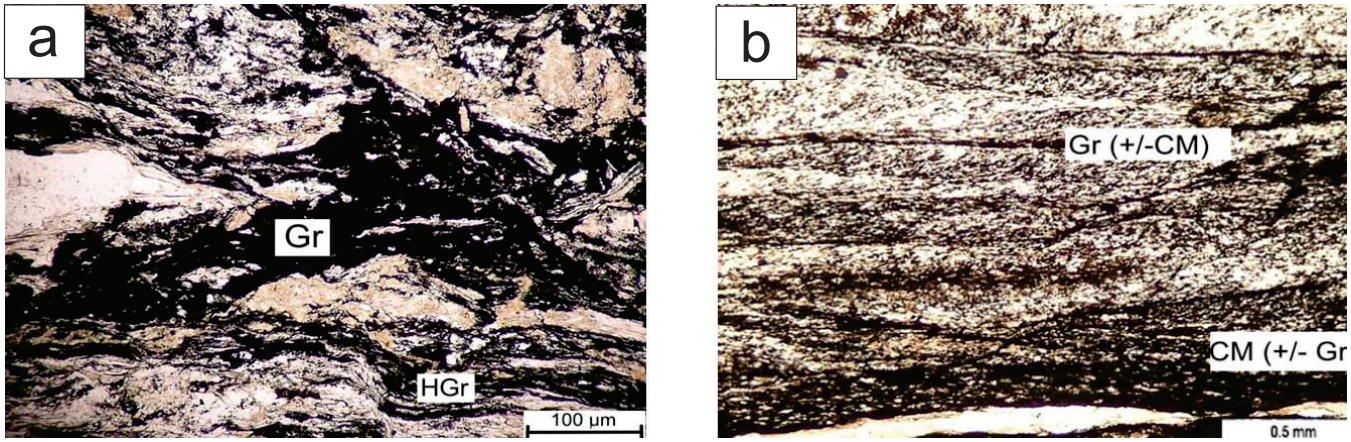


**Figure 3.** Photomicrograph of different types of carbon species in the graphitic pelitic schists (PPL Transmitted light). (A) High temperature retrograde graphite (Gr) and semi-graphite (HGr) within a high C content pelitic schists (DF60-384.2). (B) Graphite and carbonaceous matter (CM) in a medium C content pelitic schist (SW18-495.0).

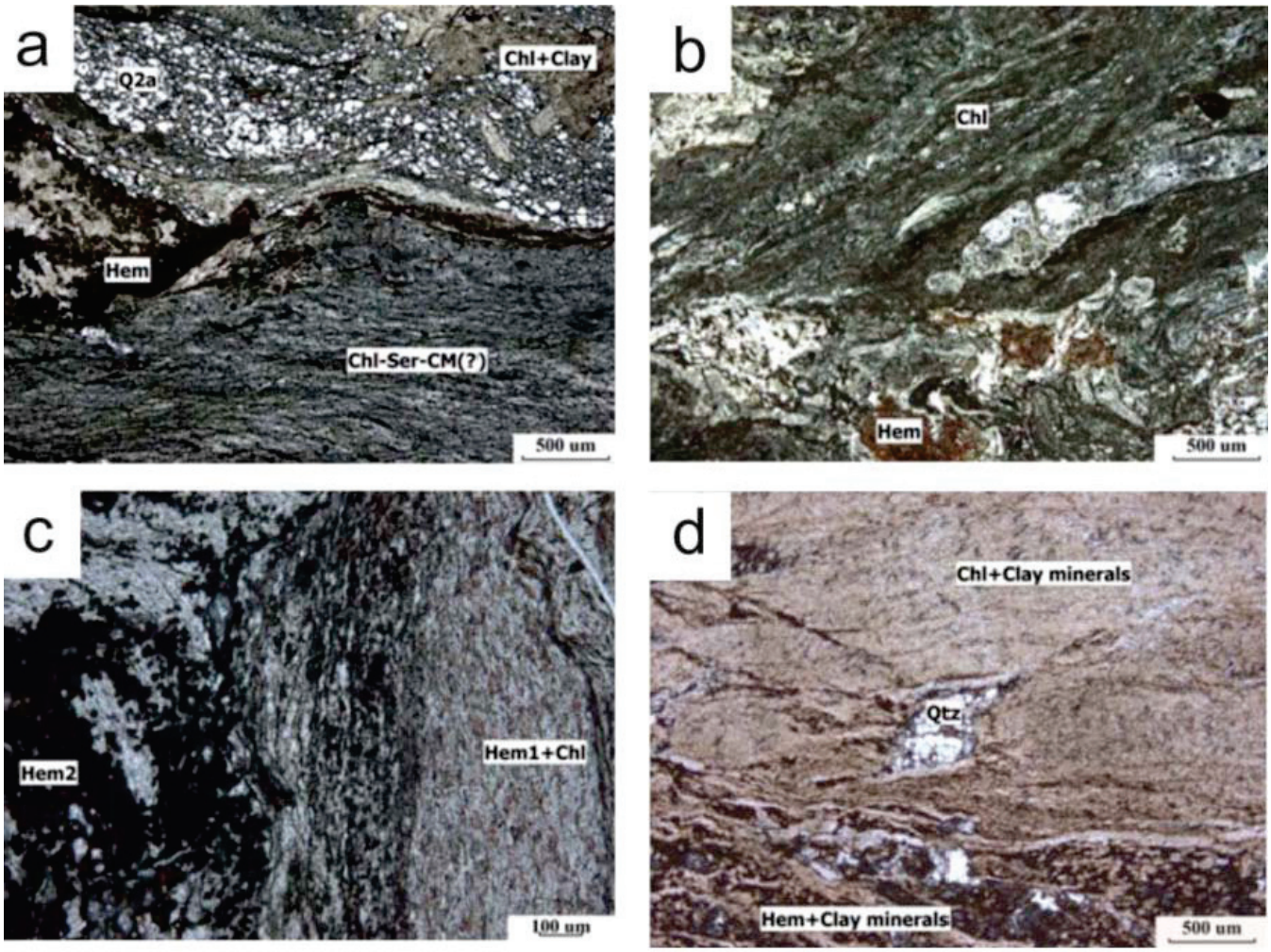


**Figure 4.** Photomicrographs of altered basement rocks (PPL Transmitted light). (A) Characteristic appearance of the RGZ with chlorite (Chl) and hematite (Hem) (SW20-380.6). (B) Green alteration (SW17-395). (C) Red alteration (SW20-381.6). (D) Bleached zone (SW18-369.9).

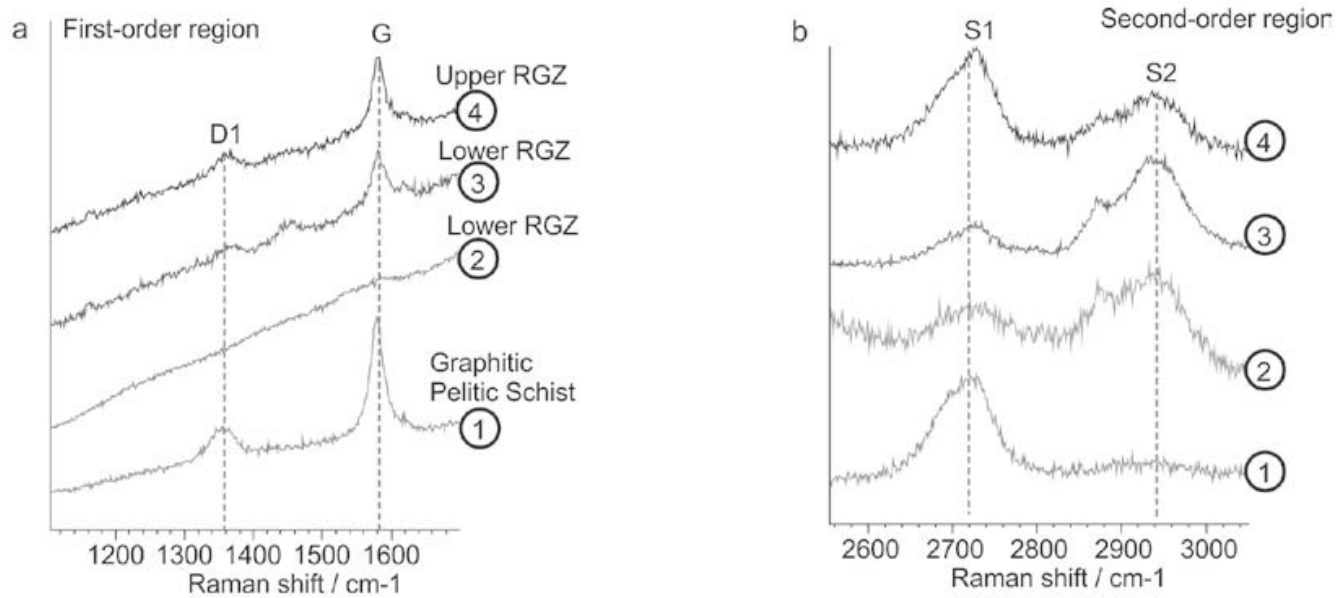


**Figure 5.** Raman spectra of carbon species in the different zones of the basement. (A) First-order region Raman spectra. (B) Second-order region Raman spectra. Spectrum 1 shows well-crystallised carbon species in the graphitic pelitic schists (SW17-415.1). Spectra 2 and 3 show low-ordered carbon species in the lower part of the RGZ (SW18-409.5, SW17-385.1, respectively). Spectra 4 show crystallised carbon species in the upper part of the RGZ (SW30-389.5).

the graphite (G) band and D1 bands in the first-order region (Fig. 5a), and in some samples the presence of an additional very weak band, D2. The second-order Raman spectra are characterized by S1 and S2 bands (Fig. 5b). Overall, the carbon species within the graphitic pelitic schists exhibit a relatively high structural organization that is typical of graphite to semi-graphite.

In the RGZ, Raman spectra are more variable. Spectra exhibiting G, D1 and D2 bands in the first-order region, and a strong Si band relative to the S2 band in the second-order region (Figs. 5a, b) are rare, and has only been identified in sample SW10-389.5 from the upper part of the RGZ (i.e. the red zone). However, this spectrum suggests that well-crystallized carbon species are present. In contrast, some spectra exhibit an indistinct G band and very wide D1 band with low intensity (Fig. 5a-spectrum 2), characteristic of amorphous carbon species. The second-order region for this sample has a S2 band which is stronger than the S1 band (Fig. 5b), which provides evidence for the presence of very weak structural organization, and is similar to spectra from bitumen (Jehlicka et al., 2003). A small peak can be present around 2880 $cm^{-1}$, associated with the S2 band, and suggests the presence of an organic compound. Overall, the samples from the RGZ have spectra with a stronger S2 band in the second-order region compared to those from the graphitic pelitic schists, indicating that the carbon-species are less well-ordered.

*Geochemistry summary*

The pelitic schists have a total carbon content that varies between 0.08 and 5.37 wt. %, which correlates with the amount of visually estimated graphite in each sample. Also, the samples exhibit a positive correlation between total carbon and total sulphur (Fig. 6a), with sulphur reflecting the pyrite content of the schists. In contrast, the samples from the RGZ, including the green zone to the red zone, and the bleached zone have low but variable carbon contents (mainly between 0.08 and 0.98 wt. %, but as high as 1.99 wt. %), whereas sulphue is completely depleted in all the altered rocks (Fig. 6a). Although the carbon content in the RGZ is sometimes similar to the lower carbon content in the variably graphitic pelitic schist, there are no samples from the RGZ that have high carbon content comparable to the variably graphitic pelitic schist. The lowest carbon content can be correlated with the loss of graphite upward into the bleached zone. The $Fe^{2+}/Fe^{3+}$ ratio is approximately 1 in the upper part of the RGZ and less than 1 in the bleached zone, whereas the lower part of the RGZ and the graphitic pelitic schists are variably reduced ($Fe^{2+}/Fe^{3+}$ >1).

Major element geochemistry of samples from the RGZ, including the green zone and the red zone, is quite similar to that of the graphitic pelitic schists. The major element composition of the green zone, in particular, is indistinguishable from the variably graphitic schists (Fig. 6). A lower $SiO_2$ content (down to 20 wt. %) and a higher MgO content (up to 16.9 wt. %) may be observed in the rocks from the RGZ and is related to the presence of pervasive chlorite alteration. In contrast, the samples from the bleached zone have higher $Al_2O_3$, $K_2O$, $TiO_2$, and $Na_2O$ contents (Figs. 6b, c, d). The sodic enrichment may result from the possible growth of fine-grained hydrothermal dravite within the clay mineral assemblage. The pelitic schists from the bleached zone are weakly mineralized (U up to 187 ppm) (Fig. 6e) with the presence of small amounts of hydrothermal uraninite along fractures. Usually, there is a close relationship between carbon and uranium (Landais, 1996), but the bleached zone and the RGZ are enriched in uranium relative to the less altered graphitic pelitic schists (Fig. 6e). Also, the samples from the

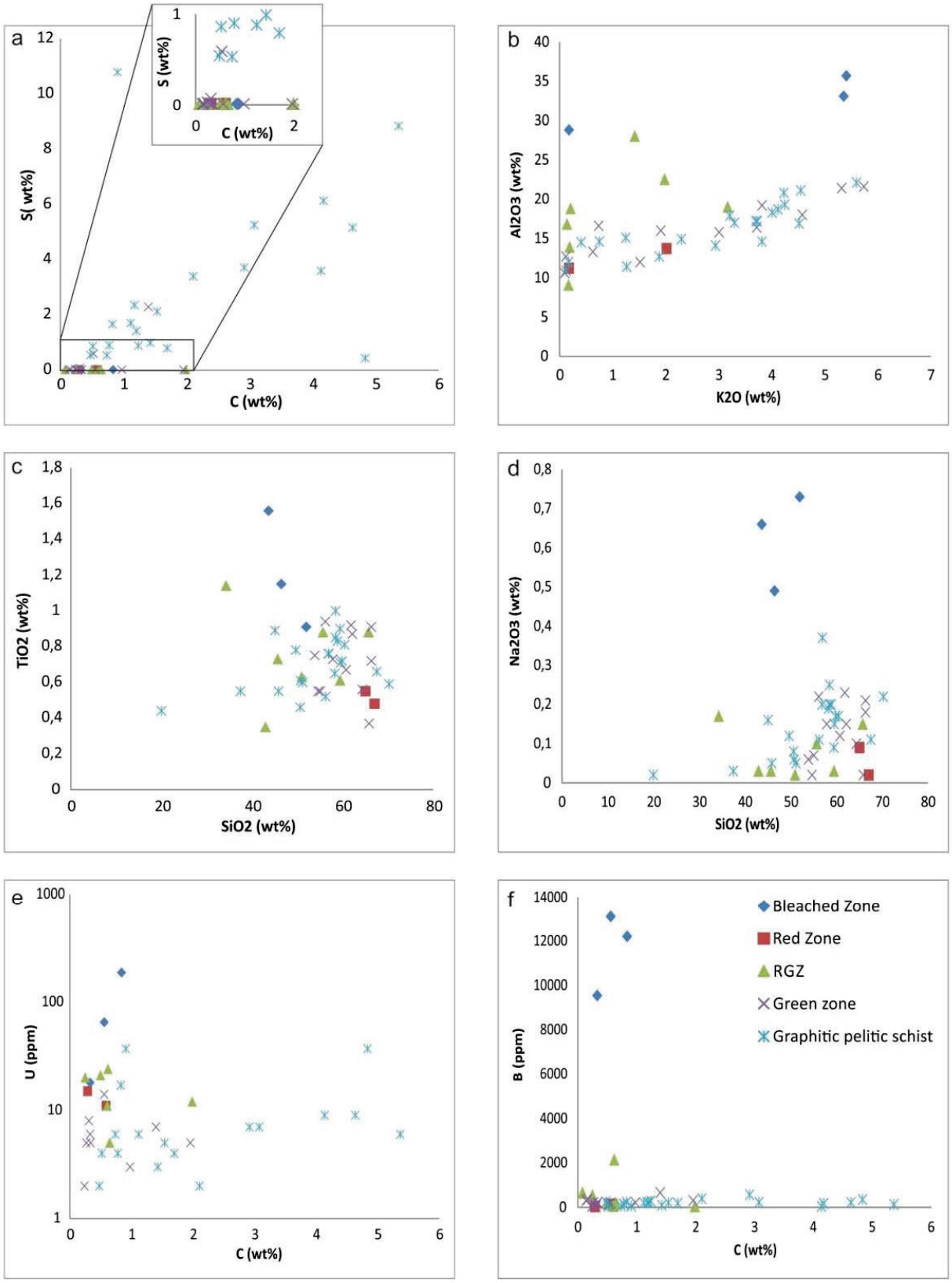


**Figure 6.** Major element composition of the graphitic and graphite depleted rocks of the different zones of the basement. The inset in (a) shows that C content is sometimes similar in the VGPS and the RGZ, but the sulphur content in the latter is always low.

bleached zone have very high boron contents (from 30 ppm to 13.100 ppm) (Fig. 6f) due to their high dravite content.

Samples from the less altered basement rocks, the RGZ, and the bleached zone have very similar chondrite normalized REE patterns. They show higher LREE content, with $(La/Yb)_N$ varying from 1.2 to 36.9, and a negative Eu anomaly. Furthermore, the HREE (total Tb to Yb)/LREE (total La to Gd) ratio is less than 1 (0.04 to 0.41). These observations are typical of the basement alteration halo associated with unconformity-type mineralization (Fayek and Kyser, 1997; Mercadier et al., 2011). Also, these chondrite-normalized REE patterns, and the presence of a well-pronounced Eu anomaly, are similar to the chondrite-normalized REE distributions found in average post-Archean shales (Condie, 1993) and to the graphitic pelitic gneisses of the basal Wollaston Group below the eastern Athabasca Basin (Madore and Annesley, 1997).

Mass-balance calculations also confirm the loss of carbon and sulphur in the RGZ, including the green zone, and the bleached zone relative to the variably graphitic pelitic schist, and a large gain of boron in the bleached zone, compared to an insignificant variation in the RGZ and the green zone (Fig. 6). The bleached zone is the zone which shows the most significant variations when compared to the other zones. The bleached zone overprints the RGZ and is therefore a younger alteration event. This alteration resulted in an enrichment of $Na_2O$, B, Cu and U, and a loss of $Fe_2O_3$, $SiO_2$ and CaO, compared to the RGZ.

*Fluid inclusion summary*

Fluid inclusion investigations were undertaken to document the characteristics of fluids that interacted with the variably graphitic pelitic schists and their equivalent graphite-depleted rocks (Pascal, 2014; Pascal et al., 2015). Several quartz generations have been identified in the basement samples (Pascal, 2014). Early quartz veins (Q1 and Q2) formed before the deposition of the Athabasca Basin, and two later quartz vein sets (Q3 and Q4) that could be related to post-Athabasca deformation and fluid flow, and therefore could potentially be related to uranium mineralization.

In the graphitic pelitic schists, monophase vapor (V) secondary fluid inclusions have been observed. They all homogenize into the vapor phase at very low temperatures (mainly between -135 and -125°C and -90 and -70°C). Raman analysis of these fluid inclusion types showed the presence of two different types of fluid; methane ($CH_4$)-dominant and nitrogen ($N_2$)-dominant fluids, with the latter having the lowest temperature of homogenization. Isochores have been determined and the range of pressure-temperature estimated for these vapour inclusions is 4.5 to 80 MPa for a temperature range of 200 to 500°C under hydrostatic regime (Pascal, 2014).

In the RGZ, aqueous two-phase (Liquid (L) + V) and three-phase (L + V + Halite) secondary fluid inclusions are the dominant type of fluid inclusions observed. The temperature of melting ice for the two-phase fluid inclusions varies between -35.5°C and -16.4°C with a dominant population between -26°C and -23°C. These temperatures indicate that salts other than NaCl are present in the fluid and are similar to those observed by Derome et al. (2005) and Mercadier et al. (2010). These temperatures yield a range of salinity between 27.4 and 19.8 wt. % equivalent NaCl-$CaCl_2$. The temperature of melting of halite in the three-phase fluid inclusions range from 190 to 240°C, which convert to a salinity varying between 31 and 34 wt. % equivalent NaCl.

## Comparison of the Characteristics of Graphite-Bearing and Graphite-Depleted Rocks

The graphitic pelitic schists and the graphite-depleted rocks are texturally very similar which suggests that the rocks were similar mineralogically before alteration occurred but some process or combination of processes removed graphite. Our analyses show that the graphite-depletion reflects fluid-rock interactions, in particular within the bleached zone, leading to gain and loss in some elements. Carbon and sulphur have been completely removed, compared to the variably graphitic pelitic schists. Several events through time could be responsible for the breakdown of graphite, carbonaceous matter and sulphides. The resulting products of the breakdown may have included carbon and sulphur as gas and/or fluid (i.e. rich in $CH_4$) which migrated upward to and above the unconformity. If the timing was appropriate these products could have played a role in uranium precipitation, as suggested by Hoeve and Sibbald (1978). However, this depletion of graphite could have started during retrograde metamorphism, continued through paleoweathering, and been completed during fluid-rock interaction with basin brines.

The presence of $CH_4$-rich fluids and $N_2$-rich fluids in coexisting fluid inclusions within quartz from the graphitic pelitic schists support interaction of these fluids with the graphitic rocks. Methane can be generated by the breakdown of graphite to $CH_4$ (Cabrera et al., 1982) during hydration reactions and/or cooling of C-O-H fluids (Huizenga, 2011; Annesley and Wheatley, 2011; Card and Annesley, 2012), and $N_2$ could have been generated by the breakdown of ammonium ($NH_4^+$)-bearing feldspar and micas (Bebout et al., 1999; Hurai et al., 2000; Sadofsky and Bebout, 2000). In the upper part of the basement, within the RGZ, where graphite is absent, brines rich in NaCl and $CaCl_2$ have been identified that are similar to those observed elsewhere in the Athabasca Basin (Derome et al., 2005; Mercadier et al., 2010). These fluids have been interpreted to be the regional basinal fluid and the evolved fluid resulting from fluid/rock interactions between the NaCl-rich brines and Ca-rich rocks of the basement, and the latter are considered to be related to uranium mineralization (Derome et al., 2005; Derome et al., 2007; Mercadier et al., 2010; Richard et al., 2010). As these fluids have circulated in the RGZ, where graphite has been lost, these fluids could also be responsible for the consumption of graphite. In this case, the fluids may have reacted with graphite and leading to its breakdown to $CH_4$ which could have acted as a reductant driving deposition of uranium. A summary of these observations is presented in figure 7.

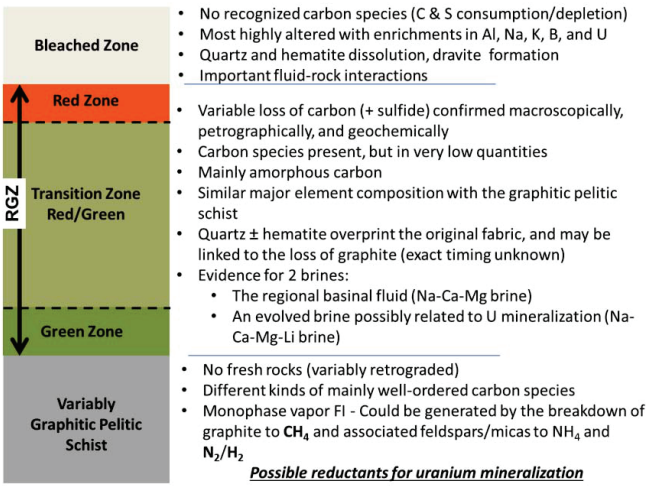


**Figure 7.** Summary of the characteristics of graphitic-bearing and graphite-depleted rocks.

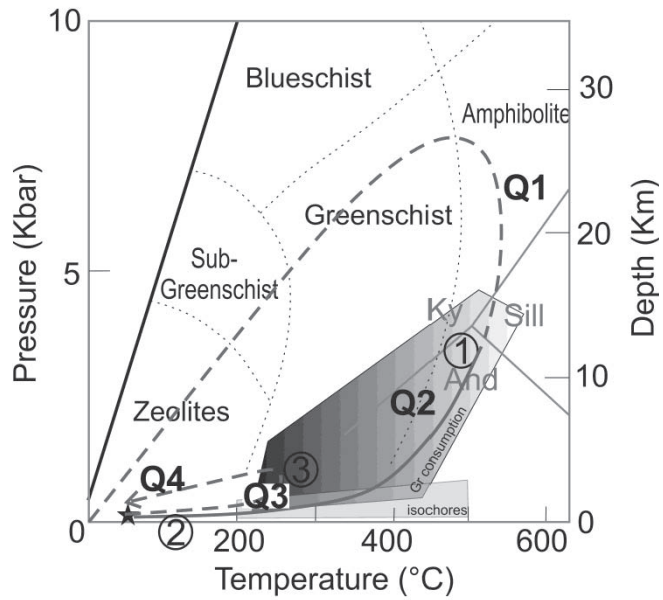


**Figure 8.** Pressure-temperature diagram illustrating the path followed by the basement rocks (long-dashed and solid line), the approximate timing of quartz generations (Q1, Q2, Q3 and Q4), fluid inclusions isochores calculated for $CH_4$ –rich and $N_2$-rich fluid inclusions (clear grey field), and the possible periods during which graphite was depleted (shaded grey field, modified after Ault and Selverstone, 2008) (1, 2, 3).

## Implications for graphite consumption and uranium exploration.

The aim of this study was to confirm and document the depletion of graphite in the basement rocks underlying the Dufferin Lake Zone in the south-central part of the Athabasca Basin, and to determine the mechanism(s) which could be responsible for this depletion. An attempt is made to relate the changes to the basement rocks along their PT-t path (Fig. 8), with the characteristics of carbon species and composition of fluid inclusions (Pascal, 2014; Pascal et al., 2015).

In summary we documented the following through PT-t space:

1. During prograde metamorphism:
   i. The original rocks, interpreted to be black shales, rich in carbonaceous (organic) matter, were metamorphosed to graphitic pelitic schists.
   ii. $NH_4^+$ may have been liberated from the carbonaceous matter and stored in K-micas. Carbonaceous matter became more ordered and crystalline (semi-graphite to graphite) as metamorphic grade increased (Beyssac et al., 2002).
   iii. Early quartz veins (Q1) formed during the peak metamorphism.
2. During retrograde metamorphism:
   i. Fluids interacted with the graphitic basement rocks, leading to the breakdown of graphite to $CH_4$ and the liberation of $NH^{4+}$ from the phyllosilicate minerals (Bottrell et al., 1988). This may have led to the formation of $N_2$ following: $2NH^{4+} \rightarrow N_2 + 8H^+$. Overall, the C-O-H fluid that formed during retrograde metamorphism and the uplift of the basement rocks may have been the one responsible for incipient, but not total, graphite consumption (Huizenga, 2011) (stage 1 – Fig. 8). In this case, these fluids would have had no role in uranium mineralization.
   ii. Pre-Athabasca quartz (Q2) veins formed.
3. Pre-Athabasca paleoweathering (stage 2 – Fig. 8): alteration of the upper part of the basement leading to the formation of the RGZ (Macdonald, 1980, 1985). Graphite and sulphides in the basement rocks may have broken down during paleoweathering leading to the release of carbon and sulphur species into the environment at this time.
4. Post-Athabasca Basin:
   i. Athabasca Basin is deposited and post-Athabasca (Q3 and Q4) veins are formed.
   ii. Post-Athabasca circulation of oxidized basinal brines with associated hydrothermal alteration (stage 3 – Fig. 8) occurred in the basement. These fluids altered the upper part of the basement (RGZ) and produced the bleached zone which overprints the regolith profile. These brines could also have reacted with graphite and sulphides in the variably graphitic schists resulting in the migration of carbon and sulphur as fluid and/or gas to the unconformity and into the sandstone, utilizing the original graphite-sulphide-rich fault structures.

Thus, several events are considered to be responsible for graphite consumption. However, graphite depletion is interpreted to be more prevalent with decreasing pressure along retrograde PT-t paths (Ault and Selverstone, 2008), and particularly near the lower temperature part of retrograde metamorphism. Therefore, the late retrograde and diagenetic hydrothermal alterations are interpreted to be the major processes that have played the most important role in the depletion/consumption of graphite. This is supported by the fact that the most altered zone, the bleached zone, has no

graphite, but contains evidence of significant fluid-rock interactions, including the one(s) that are most likely related to uranium mineralization. The interaction of fluids with early graphite led to its consumption and to the formation of $CH_4$ (as observed in the fluid inclusion study; Pascal, 2014; Pascal et al., 2015). If the timing of graphite consumption was appropriate, the upward migration of gases (and associated fluids) could have interacted with uranium-bearing oxidized basinal fluids above the unconformity and acted as a reductant for deposition of uranium. Previous studies have identified hydrocarbon buttons in the sandstone adjacent to mineralization, which suggests the migration of carbon species at the appropriate time (Hoeve and Sibbald, 1978; Landais, 1996). Recent numerical modelling by Chi et al. (2014) has shown that hydrocarbons generated in the Douglas Formation could have migrated to the unconformity and played a role in uranium mineralization. The authors further propose that (although not proven yet) the solid bitumen crosscutting uraninite could reflect hydrocarbons remaining as fluids after mineralization, flowing into fractures in the ores and forming bitumen. However, Leventhal et al. (1987), Wilson et al. (2007), and Ramaekers and Catuneanu (2013) proposed that $CH_4$ may be related to post-ore alteration of hydrocarbons derived from the overlying Douglas Formation or Western Canada sedimentary basin rocks.

This study has provided relative age constraints on the possible processes leading to the consumption of graphite in this part of the basin, although the absolute age of these processes especially with respect to the timing of uranium mineralization is still not known.

## Acknowledgments

This work forms part of a Master of Science thesis project by the senior author. The authors acknowledge the financial support of Cameco Corporation, Natural Science and Engineering Research Council of Canada through a Discovery Grant to Ansdell, and the Department of Natural Resources of Canada Targeted Geoscience Initiative Phase 4 (TGI4) Grants program. Thanks to Aaron Brown and Gary Witt (Cameco) for organizing field logistics, Kyle Reid for field support, Blaine Novakovski for preparation of thin sections, Tom Bonli for microprobe analyses, Jason Maley for his help and discussion about the Raman and the results, and Marie-Christine Boiron for training in fluid inclusion analysis and interpretation. Dan Jiricka and Tom Kotzer provided suggestions throughout the project. Gerard Zaluski is thanked for a highly constructive review of the initial draft of the manuscript and Eric Potter for the editorial handling.

## References

Annesley, I.R., and Wheatley, K., 2011. Insights into understanding the carbon-uranium (± sulfur and boron) geochemical system along a retrograde P-T-t path from 600°C to 250°C: New constraints with implications for U/C-type uranium deposits; Joint annual meeting of the Geological Association of Canada – Mineralogical Association of Canada, Abstracts, v. 34, p. 4–5.

Ault, K.A., and Selverstone, J., 2008. Microtextural constraints on the interplay between fluid–rock reactions and deformation; Contributions to Mineralogy and Petrology, v. 156, p. 501–515.

Bebout, G.E., Cooper, D.C., Bradley, A.D., and Sadofsky, S.J., 1999. Nitrogen-isotope record of fluid-rock interactions in the Skiddaw aureole and granite, English Lake District; American Mineralogist, v. 84, p. 1495–1505.

Beyssac, O., Goffé, B., Chopin, C., and Rouzaud, J.N., 2002. Raman spectra of carbonaceous material in metasediments: a new geothermometer; *Journal of Metamorphic Geology, v.* 20, p. 859–87.

Bottrell, S.H., Carr, L.P., and Dubessy, J., 1988. A nitrogen-rich metamorphic fluid and coexisting minerals in slates from North Wales; *Mineralogical Magazine, v.* 52, p. 451-457

Cabrera A.L., Heinemann, H., and Somorjai, G.A., 1982. Methane production from the catalyzed reaction of graphite and water vapor at low temperatures (500-600 K); Journal of Catalysis, v. 75, p. 7–22, doi: 10.1016/0021-9517(82)90117-8

Card, C.D., 2012. A proposed domainal reclassification for Saskatchewan's Hearne and Rae provinces; in Saskatchewan Summary of Investigations 2012; Saskatchewan Geological Survey, Miscellaneous Report 2012-4(2), p. 9.

Card, C.D., and Annesley, I.R., 2012. The origin(s) of graphite-rich rocks in the Wollaston-Mudjatik Transition Zone: syngenetic versus epigenetic?; Saskatchewan Geological Survey, Open House 2012, Abstract volume, p 6.

Card, C.D., Pana, D., Portella, P., Thomas, D.J., and Annesley, I.R. , 2007. Basement rocks to the Athabasca Basin, Saskatchewan and Alberta; in EXTECH IV: Geology and Uranium EXploration TECHnology of the Proterozoic Athabasca Basin, Saskatchewan and Alberta, (ed.), C.W. Jefferson and G. Delane; Geological Survey of Canada, Bulletin 588, p. 69–87.

Card, C.D., McEwan, B., and Bosman, S.A., 2008. The Cree Lake South Project 2008: Regional Implications of Bedrock mapping along the Virgin River Transect; in Summary of Investigations 2008, Saskatchewan Geological Survey, Miscellaneous Report 4(2), 23 p.

Chi, G., Li, Z., and Bethune, K.M., 2014. Numerical modeling of hydrocarbon generation in the Douglas Formation of the Athabasca Basin (Canada) and implications for unconformity-related uranium mineralization; Journal of Geochemical Exploration, v. 144, p. 37–48

Condie, K.C., 1993. Chemical composition and evolution of the upper continental crust: Contrasting results from surface samples and shales; Chemical Geology, v. 104, p. 1–37.

Cuney, M., Brouand, M., Cathelineau, M., Derome, D., Freiberger, R., Hecht, L., Kister, P., Lobaev, V., Lorilleux, G., Peiffert, C., and Bastoul, A.M., 2003. What parameters control the high grade-large tonnage of the Proterozoic unconformity related uranium deposit?; in Uranium Geochemistry 2003, International Conference, Proceedings, (ed.) M. Cuney; Unité Mixte de Recherche CNRS 7566G2R, Université Henri Poincaré, Nancy, France, p. 123–126.

Derome, D., Cathelineau, M., Cuney, M., Fabre, C., and Lhomme, T., 2005. Evidences of brine mixings in the McArthur River unconformity-type uranium deposit (Saskatchewan, Canada). Implications on genetic models; Economic Geology v. 100, p. 1529–1545.

Derome, D., Cathelineau, M., Fabre, C., Boiron, M.-C, Banks, D., Lhomme, T., and Cuney, M., 2007. Reconstitution of paleo-fluid composition by Raman, LIBS and crush-leach techniques: application to mid-proterozoic evaporitic brines (Kombolgie formation basin, northern territories, Australia); Chemical Geology, v. 237, p. 240–254.

Fayek, M., and Kyser, T.K., 1997. Characterization of multiple fluid-flow events and rare-earth-element mobility associated with formation of unconformity-type uranium deposits in the Athabasca Basin, Saskatchewan; The Canadian Mineralogist, v. 35, p. 627–658.

Gilboy, C.F., 1985a. Basement geology, part of the Cree Lake (south) area; Saskatchewan Energy and Mines, Report 203, 1-47.

Gilboy, C.F., 1985b. Compilation bedrock Geology, Cree Lake, NTS Area 74G; Saskatchewan Energy and Mines, Report 237.

Hoeve, J., and Sibbald, T., 1978. On the Genesis of Rabbit Lake and Other Unconformity-type Uranium Deposits in Northern Saskatchewan, Canada; Economic Geology, v. 73, p. 1450–1473.

Hoffman, P.F., 1990. Subdivision of the Churchill Province and extent of the Trans-Hudson orogeny; in The Early Proterozoic Trans-Hudson Orogen of North America, (eds.) J.F. Lewry and M.R. Stauffer; Geological Association of Canada, Special Paper 37, p. 15–39.

Huizenga, J.M., 2011. hermodynamic modelling of a cooling C–O–H fluid–graphite system: implications for hydrothermal graphite precipi-

tation; Mineralium Deposita, v. 46, p. 23–33.

Hurai, V., Janak, M., Ludhova, L., Horn, E.E., Thomas, R., and Majzlan, J., 2000. Nitrogen-bearing fluids, brines and carbonate liquids in Variscan migmatites of the Tatra Mountains, Western Carpathians; heritage of high-pressure metamorphism; European Journal of Mineralogy, v. 12, p. 1283–1300.

Jefferson, C.W., Thomas, D.J., Gandhi, S.S., Ramaekers, P., Delaney, G., Brisbin, D., Cutts, C., Portella, P., and Olson, R.A., 2007. Unconformity associated uranium deposits of the Athabasca Basin, Saskatchewan and Alberta; in EXTECH IV: Geology and Uranium EXploration TECHnology of the Proterozoic Athabasca Basin, Saskatchewan and Alberta, (ed.) C.W. Jefferson and G. Delaney; Geological Survey of Canada, Bulletin 588, p. 23–67.

Jehlicka, J., Urban, O., and Pokorny, J., 2003. Raman spectroscopy of carbon and solid bitumens in sedimentary and metamorphic rocks; Spectrochimica Acta Part A, v. 59, p. 2341–2352.

Jiricka, D.E., Witt, G., and Fiolleau, K., 2007. Southwest Athabasca Project; 2006 annual exploration report, Internal Cameco Corporation report, p. 1–77.

Landais, P., 1996. Organic geochemistry of sedimentary uranium ore deposits; Ore Geology Reviews v. 11, p. 33–51.

Leventhal, J.S., Grauch, R.I., Threlkeld, C.N., and Lichte, F.E., 1987. Unusual organic matter associated with uranium from the Claude deposit, Cluff Lake, Canada; Economic Geology, v. 82, p. 1169–1176.

Macdonald, C., 1980. Mineralogy and geochemistry of a Precambrian regolith in the Athabasca Basin; unpublished M.Sc. thesis: University of Saskatchewan, 151 p.

Macdonald, C., 1985. Mineralogy and geochemistry of the sub-Athabasca regolith near Wollaston Lake; in Geology of Uranium Deposits, Proceedings of the CIM-SEG Uranium Symposium, (ed.) T.I.I. Sibbald and W. Petruk; The Canadian Institute of Mining, Metallurgy and Petroleum, v. 32, p. 155–158.

Madore, C., and Annesley, I.R., 1997. Graphitic pelitic gneisses of the paleoproterozoic Wollaston Group, Hearne Province, Saskatchewan; in Mineral deposits, Research and Exploration- Where do they meet? (ed.) H. Papunen and H. Balkema, p. 79–82.

Mercadier, J., Cuney, M., Cathelineau, M., and Lacorde, M., 2011. U redox fronts and kaolinisation in basement-hosted unconformity-related U ores of the Athabasca Basin (Canada): late U remobilization by meteoric fluids; Mineralium Deposita, v. 46, p. 105–135.

Mercadier, J., Richard, A., Boiron, M.-C., Cathelineau, M., and Cuney, M., 2010. Migration of brines in the basement rocks of the Athabasca Basin through microfracture networks (P-Patch U deposit, Canada); Lithos, v. 115, p. 121–136.

Pascal, M., 2014. Graphite-bearing and graphite-depleted basement rocks in the Dufferin Lake Zone, south-central Athabasca Basin, Saskatchewan; unpublished M.Sc. thesis, University of Saskatchewan, Saskatoon, Canada, 193 p (http://hdl.handle.net/10388/ETD-2014-07-1628).

Pascal, M., Boiron, M.-C., Ansdell, K., Annesley, I.R., Kotzer, T., Jiricka, D., and Cuney, M., 2015. Fluids preserved in variably altered graphitic pelitic schists in the Dufferin Lake zone, south-central Athabasca Basin, Canada: Implications for graphite loss and uranium deposition; Mineralium Deposita (in revision after review).

Powell, B., Wood, G., and Bzdel, L., 2007. Advances in Geophysical Exploration for Uranium Deposits in the Athabasca Basin; in Proceedings of Exploration 07: Fifth Decennial International Conference on Mineral Exploration, (ed.) B. Milkereit; p. 771–790.

Ramaekers, P. and Catuneanu, O., 2013. Rifting and the generation and modification of Athabasca Basin uranium deposits; Saskatchewan Geological Survey Open House 2013. http://economy.gov.sk.ca/Technical%20Session%201%20Uranium%20Geoscience

Richard, A., Pettke, T., Cathelineau, M., Boiron, M.-C., Mercadier, J., Cuney, M., and Derome, D., 2010. Brine–rock interaction in the Athabasca basement (McArthur River U deposit, Canada): consequences for fluid chemistry and uranium uptake; Terra Nova, v. 22, p. 303–308.

Sadofsky, S.J., and Bebout, G.E., 2000. Ammonium partitioning and nitrogen-isotope fractionation among coexisting micas during high-temperature fluid-rock interactions; examples from the New England Appalachians; Geochimica et Cosmochimica Acta, v. 64, p. 2835–2849

Thomas, D., Matthews, R.B., and Sopuck, V., 2000. Athabasca Basin (Canada) unconformity-type uranium deposits: exploration model, current mine developments and exploration directions; in Geology and Ore Deposits 2000: The Great Basin and Beyond, (ed.) J.K. Cluer, J.G. Price, E.M. Struhsacker, R.F. Hardyman and C.L. Morris; Geological Society of Nevada, Symposium Proceedings, v. 1, p. 103–126.

Wallis, R.H., 1970. The geology of the Dufferin Lake Area (West Half) Saskatchewan; Department of Mineral Resources, Geological Sciences Branch, Precambrian Geology Division (Regina), Geological Report 132.

Wilson, N.S.F., Stasiuk, L.D., and Fowler, M.G., 2007. Origin of organic matter in the Proterozoic Athabasca Basin of Saskatchewan and Alberta, and significance to unconformity uranium deposits; in EXTECH IV: Geology and Uranium Exploration TECHnology of the Proterozoic Athabasca Basin, Saskatchewan and Alberta, (ed.) C.W. Jefferson and G. Delaney; Geological Survey of Canada, Bulletin 588, p. 325–339.